

Kinesin swivels to permit microtubule movement in any direction

ALAN J. HUNT AND JONATHON HOWARD*

Department of Physiology and Biophysics, SJ-40, University of Washington, Seattle, WA 98195

Communicated by A. J. Hudspeth, September 9, 1993 (received for review August 9, 1993)

ABSTRACT Kinesin is a motor protein that uses the energy derived from ATP hydrolysis to transport organelles along microtubules. By analyzing the thermal fluctuation of microtubules tethered to glass surfaces by single molecules of kinesin, we have measured the torsional flexibility of the motor protein. The torsional stiffness of kinesin, $(117 \pm 19) \times 10^{-24}$ N·m·rad⁻¹ (mean \pm SEM), is so low that one *kT* of energy ($\approx 4.1 \times 10^{-21}$ J at room temperature) is sufficient to twist a kinesin molecule through more than 360° from its resting orientation. Consistent with this flexibility, motility assays show that one or more kinesin molecules can move a microtubule equally well in any direction. These results explain how a motor on the surface of an organelle can rapidly bind to and capture a microtubule irrespective of the organelle's orientation. Furthermore, the flexibility ensures that several motors can efficiently work together even though they are randomly oriented on the surface of an organelle rather than being in precise arrays like the motors of muscle and cilia.

Cellular motility is mediated by motor proteins such as myosin, dynein, and kinesin. These proteins use energy derived from ATP hydrolysis to drive a cyclical reaction in which they bind to, exert force against, and release from their associated cytoskeletal filaments—actin filaments in the case of myosin and microtubules in the cases of dynein and kinesin. In muscle and cilia, the myosin and dynein motors are contained in oriented arrays that ensure precise alignment between the motors and the filaments. On the other hand, cytoplasmic motors such as kinesin (1, 2) are not precisely arrayed on the surfaces of the organelles. This poses a number of potential problems. First, the rate at which an organelle can latch on to a filament might be prohibitively low if the organelle as a whole has to rotate for the motor and its binding site on the filament to become stereospecifically aligned. Second, if each motor can interact with a filament over only a restricted range of angles, then only a small fraction of randomly oriented motors will be able to work simultaneously to move the organelle along the filament.

It is clear that both of these problems are solved if the motor is flexible: if the motor molecule has a region of high torsional flexibility between its organelle-binding domain and its filament-binding domain then filament binding and force generation ought to depend only weakly on the angle between the organelle and the filament. Conversely, if binding and force generation are insensitive to angle then there must exist a high degree of torsional flexibility to permit stereospecific binding to the filament.

Two disparate observations indicate that kinesin may indeed be flexible. First, kinesin possesses a region of high susceptibility to proteolysis. Kinesin contains two globular head domains at one end of a coiled-coil rod, and a tail domain at the other; the heads bind microtubules and ATP, and the tail is thought to bind organelles (3–8). Limited proteolysis produces a 45-kDa head fragment that retains the microtubule

and ATP-binding activity but does not support motility (4, 6). By analogy to myosin (9–13) and immunoglobulin G (e.g., ref. 14), susceptibility to proteolysis suggests that a flexible hinge region exists between each of kinesin's heads and the rod domain. The second observation is from motility assays. As a microtubule is translated in the direction of its long axis by a single kinesin molecule adsorbed to a glass surface, the microtubule also rotates erratically about a vertical axis through the fixed point on the surface at which the kinesin motor is located (ref. 15; see also Fig. 5A).

In this paper we have directly measured the torsional flexibility of kinesin as well as the angular dependence of kinesin-driven motility. Both measurements strongly support a mechanical model in which the motor swivels almost freely to permit its load, the organelle, to spin or twist at will as the motor carries it along the microtubule.

METHODS

Preparation. All observations were made in 75- μ m-deep perfusion chambers bounded at the bottom by a glass microscope slide and on top by a coverglass (15, 16). The standard buffer solution contained 80 mM Pipes, 1 mM EGTA, and 2 mM MgCl₂ and was adjusted to pH 6.9 with KOH. All reagents were obtained from Sigma. The molar ratio of the light subunits to the heavy subunits of the kinesin purified from bovine brain (16) was 0.85, consistent with mole fractions of 0.85 of kinesin in the tetrameric form ($\alpha_2\beta_2$) and 0.15 in the dimer form (α_2). The glass surfaces were precoated by introducing casein at 2.5 mg/ml in standard buffer solution into the chamber. Kinesin was diluted into standard buffer solution augmented with casein at 250 μ g/ml and then introduced at 5–53 ng/ml for nucleotide-free assays (Figs. 2–4), and at 214 ng/ml in motility assays (Fig. 5). These concentrations correspond to surface densities of 0.3–3 and 13 molecules per μ m², respectively, assuming complete adsorption of kinesin to the glass surfaces during the 5 min allowed for adsorption.

Both fluorescently labeled (17) and unlabeled microtubules were polymerized from phosphocellulose-purified bovine brain tubulin (15, 16) and diluted to ≈ 0.1 mg/ml in standard buffer solution augmented with 10 μ M taxol (Drug Synthesis and Chemistry Branch, National Cancer Institute, Bethesda, MD) to prevent depolymerization. To remove the GTP used during microtubule polymerization, the diluted microtubules were pelleted and resuspended three times in standard buffer augmented with taxol, resulting in an estimated final GTP concentration of less than 10 pM. Before introduction into perfusion chambers, the microtubules were triturated to lengths of 1–5 μ m by passing the solution through a 30-gauge needle. After introduction of the microtubules, the ends of the perfusion chambers were sealed with grease to prevent fluid flow due to evaporation. Microtubules were specifically bound to kinesin molecules; as the kinesin density on the surface was decreased the density of microtubules bound to the surface also decreased. No binding occurred in the

The publication costs of this article were defrayed in part by page charge payment. This article must therefore be hereby marked "advertisement" in accordance with 18 U.S.C. §1734 solely to indicate this fact.

*To whom reprint requests should be addressed.

absence of kinesin even after 2 hr. All experiments were performed at room temperature (25–30°C). The temperature of some perfusion chambers was measured by using 50- μm -diameter T-type thermocouple wire (Physitemp Instruments, Clifton, NJ). We estimated that illumination by the 100-W mercury arc lamp raised the temperature in the observation field by less than 1°C. Images were acquired with a silicon-intensified-target camera (Hamamatsu C2400-8; Bartels & Stout, Bellevue, WA) and recorded with a 1/2-inch video-cassette recorder (Panasonic AG-7350; Proline, Seattle).

Data Analysis. The orientation of microtubules was measured either directly from recorded video images by using a protractor or by analysis of microtubule coordinates digitized by using Measure hardware (M. Walsh Electronics, San Dimas, CA) and software generously provided by S. Block (Rowland Institute, Cambridge, MA; described in ref. 18). Digitized images were corrected for field distortions in the camera. The speed of translation and its standard error were determined by linear regression. One-sided power spectra were estimated from Fourier transforms of the angle versus time data, using a rectangular window and the Mathematica software package (Wolfram Research, Champaign, IL). The power spectrum shown in Fig. 2B was smoothed at higher frequencies by convolving with a 3- to 9-point triangle window. All nonlinear least-squares fits were made by using the Marquardt–Levenberg algorithm implemented in the SigmaPlot scientific graphics package (Jandel, Corte Madera, CA). Errors are SEM.

Measurement of the Rotational Drag Coefficient. The rotational drag coefficient (Γ) was deduced from the rotational diffusion coefficient (D) by means of Einstein's relation (Eq. 2). In the absence of ATP, the mean-squared angular deviation over time intervals, $\Delta t = mt_s$ ($m = 1, 2, 4, 8, 16,$ and 32), was calculated from the time series of the angle $\phi(it_s)$ ($i = 1, \dots, N$ and t_s is the sampling interval, which was 0.5 or 1 s) by using

$$\langle \Delta\phi^2(\Delta t) \rangle = (1/n) \sum_{j=1}^{j=n} \{ \phi[m(j+1)t_s] - \phi[mjt_s] \}^2,$$

where $n = N/m - 1$. In the case of the thermal fluctuation of a damped spring, this procedure for measuring D is valid only if Δt is much less than the relaxation time, τ . For the microtubules of Fig. 3 this condition was met ($\Delta t \leq 16$ s, $\tau \geq 125$ s).

This procedure could not be used to analyze the angular fluctuation during ATP-induced translation; L_1 and L_2 (see Fig. 1A) are steadily changing due to the translation and therefore, in accordance with Eq. 4, so too does the rotational drag coefficient steadily change. Instead, the drag per unit length (c_L) was calculated by linear regression from $\langle \Delta\phi^2 \rangle = 6(1/c_L) \Delta t kT (L_1^3 + L_2^3)^{-1}$, which follows from Eqs. 2–4. Δt was chosen small enough that $L_1^3 + L_2^3$ did not change by more than 8%.

RESULTS

To measure the torsional flexibility of kinesin we tethered microtubules to a glass surface, each by means of a single kinesin molecule (Fig. 1A), and we observed their thermal motion by fluorescence (Fig. 1B) or darkfield (Fig. 2A) microscopy in the absence of ATP. Quite surprisingly, each tethered microtubule underwent as many as four complete rotations over a period of several minutes (e.g., Fig. 2A). This shows that the motor protein is extremely flexible.

But the molecule examined in Fig. 2A was not an infinitely compliant swivel, since the power spectral density (Fig. 2B) did not increase indefinitely as the frequency decreased. Instead, the power spectrum leveled off at low frequency. This asymptotic behavior is consistent with kinesin behaving like a torsional spring with nonzero stiffness, K (stiffness is the

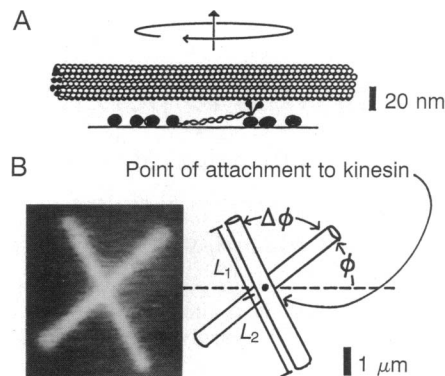


FIG. 1. A microtubule exhibits thermally driven rotations around its point of attachment to a single kinesin molecule. (A) A single kinesin molecule forms a tether between a microtubule and a glass surface that has been coated with casein (globular objects). The figure is drawn approximately to scale except that the microtubules were approximately 10 times longer. (B) Two fluorescence images of a microtubule bound to a kinesin molecule are superimposed to show rotation. The drawing on the right defines lengths and angles used in the text.

reciprocal of flexibility), that is excited into diffusive, torsional motion by thermal torques (M). In other words, the kinesin–microtubule complex may be described by the equation

$$M = K\phi + \Gamma d\phi/dt, \quad [1]$$

where ϕ is the angle of the microtubule (in radians) and Γ is the rotational drag coefficient (19). Mass is ignored because of the low Reynolds number. The power spectrum predicted by this

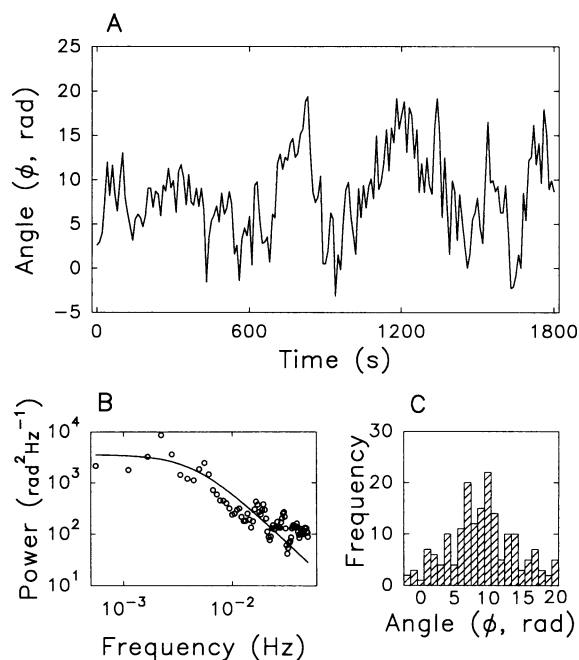


FIG. 2. (A) The angle of a kinesin-tethered microtubule observed by darkfield microscopy varies with time. This microtubule underwent more than 3.5 complete rotations. The angle was measured every 10 s. $L_1 = 0.35 \mu\text{m}$ and $L_2 = 1.35 \mu\text{m}$. (B) The one-sided power spectrum of the data shown in A. At low frequencies the spectral density of the microtubule angle is less than expected for unbounded diffusion. This indicates that the flexibility is not infinite. The line indicates the least-squares fit to the data of the Lorentzian: $P(f) = 4kT\Gamma[1 + (2\pi f\tau)^2]^{-1}$, where $P(f)$ is the power at frequency f and the other symbols are defined in the text. (C) Histogram showing the distribution of angles for the data in A.

model fit the data well (solid curve in Fig. 2B) if the torsional stiffness, K , was $(165 \pm 20) \times 10^{-24} \text{ N}\cdot\text{m}\cdot\text{rad}^{-1}$ and the drag coefficient, Γ , was $(6.0 \pm 1.3) \times 10^{-21} \text{ N}\cdot\text{m}\cdot\text{rad}^{-1}\cdot\text{s}$. The relaxation time constant ($\tau = \Gamma/K$) was $36 \pm 7 \text{ s}$. The rotational diffusion of the microtubule appears to be limited by a torsional spring rather than a pair of stops, because the distribution of angles occupied during the rotational motion resembled a Gaussian rather than a uniform distribution (Fig. 2C).

We measured the drag coefficient and the torsional stiffness of several kinesin-microtubule complexes. Γ was determined from the rotational diffusion of microtubules during time intervals much shorter than the relaxation time (Fig. 3A). The principle of the method is that, over short time intervals $\Delta t \ll \tau$, the motion is diffusive with diffusion coefficient given by Einstein's relation:

$$D = kT/\Gamma, \quad [2]$$

where k is the Boltzmann constant and T is the absolute temperature. The diffusion coefficient in turn is measured from the mean square of the change in microtubule angle over the time interval:

$$D = \langle \Delta\phi^2 \rangle / 2\Delta t, \quad [3]$$

Fig. 3A shows that the diffusion coefficient measured in this way was independent of the particular time interval Δt as expected for a diffusive process. Γ was then calculated by using Eq. 2. Γ depended on a microtubule's length (Fig. 3B), and was well fit by the relation

$$\Gamma = \frac{1}{3}c_{\perp}(L_1^3 + L_2^3), \quad [4]$$

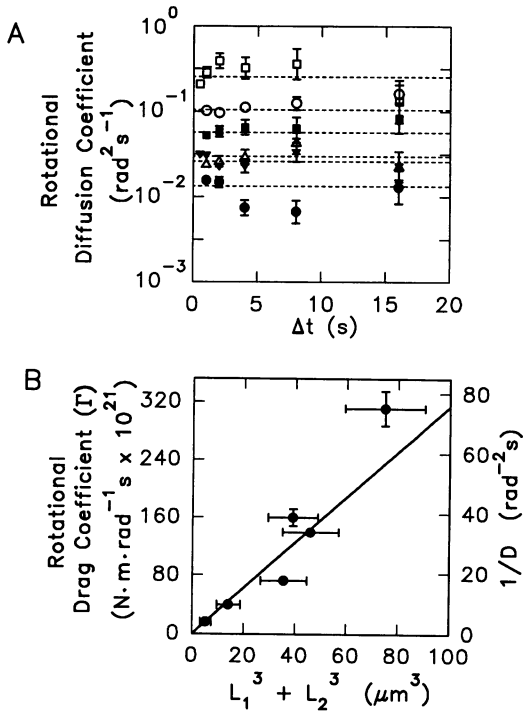


FIG. 3. (A) The rotational diffusion coefficient was independent of the time interval Δt for which it was calculated. Different symbols indicate data from different kinesin-microtubule complexes. The broken lines indicate the weighted means. The relative errors (standard error divided by the mean) correspond to $[2/(N-1)]^{-1/2}$ where N is the number of measurements used to calculate the data point. (B) The rotational drag coefficient (Γ) is proportional to the sum of the third powers of the microtubule lengths, $L_1^3 + L_2^3$, defined in Fig. 1B.

where L_1 and L_2 are lengths defined in Fig. 1B, and $c_{\perp} = 9.4 \pm 1.0 \text{ mN}\cdot\text{s}\cdot\text{m}^{-2}$ is the drag coefficient per unit length for translation perpendicular to the microtubule axis (20). Eq. 4 is derived by integrating the torque over the length of the pivoting microtubule.

The torsional stiffness was deduced from the variance of microtubule angles. For microtubules observed over long times, the variance in ϕ fell significantly below the values expected for free diffusion (Fig. 4). Since the microtubules were in thermal equilibrium with the surrounding fluid (see Discussion), the asymptotic value of the variance was used to estimate the torsional stiffness by the equipartition theorem: $\frac{1}{2}K\cdot\text{variance} = \frac{1}{2}kT$ (21). The torsional stiffness was estimated for the five microtubules recorded for the longest times. The values were consistent with each other ($\chi^2 = 5.2$, $\text{df} = 4$, $P > 0.2$) and independent of a microtubule's length, as expected if the torsional stiffness were an invariant intrinsic property of a kinesin molecule. The weighted mean was $(117 \pm 19) \times 10^{-24} \text{ N}\cdot\text{m}\cdot\text{rad}^{-1}$. The nonzero torsional stiffness implies that in the absence of ATP kinesin does not dissociate from a microtubule for a long enough time to unwind; we estimate the unwinding time to be on the order of 1–10 μs if kinesin is modeled as a slender cylinder rotating axially (20).

The torsional flexibility of kinesin is great enough to explain the erratic rotation of microtubules translating in the presence of ATP (Fig. 5A). The rotational drag coefficient of translating microtubules in the presence of ATP was not significantly different from that of tethered microtubules in the absence of ATP: the drag coefficients per unit length were $11.9 \pm 1.1 \text{ mN}\cdot\text{s}\cdot\text{m}^{-2}$ and $9.4 \pm 1.0 \text{ mN}\cdot\text{s}\cdot\text{m}^{-2}$, respectively (27°C). This indicates that the swiveling motion is still present during translation and is independent of forward motion: the energy from ATP hydrolysis is not driving the rotations observed during translation. It is possible that kinesin unwinds during that part of the reaction cycle when it is detached from the microtubule; this would allow kinesin to behave even more like a perfect swivel when ATP is present. If such unwinding does occur, the motor must still swivel to adapt to the microtubule's orientation to rebind and continue the cycle.

The similarity of the drag coefficients with and without ATP indicates that the geometry of kinesin-bound microtubules is independent of ATP. If a microtubule is modeled as a straight slender cylinder of radius $r = 15 \text{ nm}$ (22) whose surface is height b above an infinite planar surface, then the drag coefficient is predicted to be $c_{\perp} = 4\pi\eta[\text{arccosh}(1 + b/r)]^{-1}$ (23), where η is viscosity ($0.851 \text{ mN}\cdot\text{s}\cdot\text{m}^{-2}$ at 27°C).

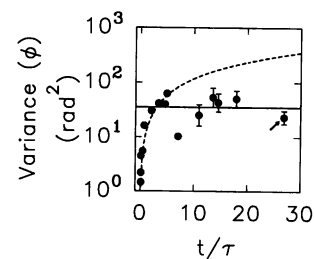


FIG. 4. Variance of the microtubule angle (ϕ) versus the total observation time (t). The observation time was normalized by the relaxation time constant (τ) to facilitate the comparison of microtubules of different lengths. For each microtubule, τ was estimated by $c_{\perp}(L_1^3 + L_2^3)/3K$, with $c_{\perp} = 9.4 \text{ mN}\cdot\text{s}\cdot\text{m}^{-2}$ and $K = 117 \times 10^{-24} \text{ N}\cdot\text{m}\cdot\text{rad}^{-1}$. The error bars associated with the five microtubules observed for greater than 10 relaxation times correspond to relative errors of $[(t/\tau - 1)/2]^{-1/2}$. The solid line shows the average variance of these same five microtubules. The point indicated by the arrow was determined from the data shown in Fig. 2. The broken line shows the behavior expected for unbounded diffusion: $\text{variance} = (kT/3K)/\tau$.

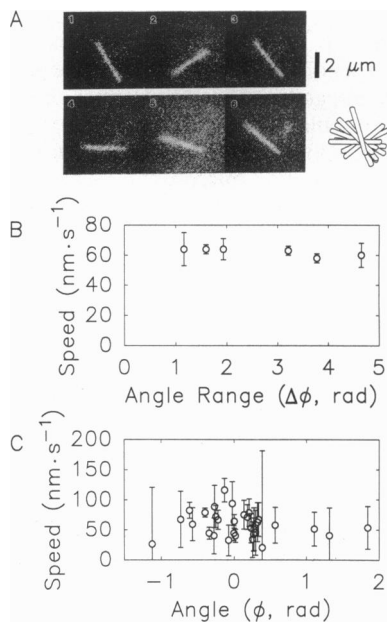


FIG. 5. The speed at which kinesin translates a microtubule is independent of the microtubule's angle. (A) Video images at 4-s intervals of a fluorescently labeled microtubule being translated by a single kinesin molecule in the presence of $3.3 \mu\text{M}$ ATP. This ATP concentration, which is about one-tenth that needed for maximum translation speed (15), was chosen so that a greater range of angles could be observed before the trailing end of the microtubule reached the kinesin molecule and the microtubule detached from the surface. At the right are overlaid traces of this same microtubule at 2-s intervals. (B) Average speed that a microtubule was translated by a kinesin molecule plotted against the range of the angles subtended by the microtubule during the translation. (C) Relation between the speed of microtubule translation and the angular deviation from the microtubule's average orientation. The data are from the same six microtubules used in B.

The measured drag coefficients correspond to heights of $6.5 \pm 1.3 \text{ nm}$ and $10.7 \pm 2.6 \text{ nm}$ in the presence and absence of ATP, respectively. In view of the $\approx 8\text{-nm}$ thick layer of casein on the glass surface (Fig. 1A), these distances agree reasonably well with the $17 \pm 2 \text{ nm}$ crossbridge distance between an organelle and the surface of a microtubule estimated from electron micrographs of axoplasm (24).

The observation that kinesin is highly flexible suggests that the relative orientation of a kinesin molecule should have little effect on its ability to bind to, exert force against, or move along a microtubule. Consistent with this, we found that orientation had no significant effect on the translation of microtubules driven by single kinesin molecules. First, microtubule translation by a single kinesin molecule was always directed along a microtubule's long axis (Fig. 5A). Second, the average speed of microtubule translation was independent of the range of angles adopted during the motion (Fig. 5B). If there were an optimal orientation, we would expect the microtubules that underwent the larger angular fluctuations to translate more slowly. Third, the speed of a moving microtubule did not decrease as it deviated from its average orientation (Fig. 5C); even for deviations as great as 90° we can rule out the possibility that the speed decreased by 31% or more at the 0.05 confidence level. Fourth, we observed a microtubule, apparently translated by two kinesin molecules, which, after its trailing end overran and detached from the trailing motor (motor 1), diffusively rotated 180° around its leading point of attachment (motor 2) and reattached to what had been the trailing motor but was now the leading motor. The microtubule then continued to travel at the same speed but now in the opposite direction (speed = 0.068 ± 0.006

$\mu\text{m}\cdot\text{s}^{-1}$ before rotation, $0.071 \pm 0.007 \mu\text{m}\cdot\text{s}^{-1}$ after rotation). When the microtubule's trailing end overran and detached from the trailing motor (now no. 2), it then diffusively rotated back through 180° and moved in the original direction. Thus the microtubule was translated equally quickly before and after both of the translating kinesin molecules had rotated through 180° .

DISCUSSION

By analyzing the thermal fluctuation of microtubules tethered to single kinesin molecules, we have made the first (to our knowledge) quantitative measurement of the torsional flexibility of a motor protein. The torsional stiffness of (117 ± 19) $\times 10^{-24} \text{ N}\cdot\text{m}\cdot\text{rad}^{-1}$ (mean \pm SEM) is so low that one kT of energy ($\approx 4.1 \times 10^{-21} \text{ J}$ at room temperature) is sufficient to twist a kinesin molecule through more than 360° from its resting orientation. Consistent with this extreme flexibility, we found that kinesin is able to translate a microtubule equally quickly in any direction—this means that the orientation of the microtubule completely dictates the direction of its translation in motility assays (the microtubule's minus end always leads).

Before accepting these measurements it is necessary to establish two points. First, the measured fluctuations are of thermal origin as shown by the following three arguments. (i) In the absence of added nucleotides, the ATP and GTP concentrations were both less than 500 pM , too low for the fluctuations to be driven by nucleotide hydrolysis. (ii) By sealing the perfusion chambers we prevented fluid evaporation, and no fluid flow leading to artifactual microtubule rotation was detectable. (iii) The measurement errors arising from digitization were small and did not contribute a significant systematic error. Second, the compliance almost certainly lies within the kinesin molecule itself rather than in the casein used to coat the glass surface. This is because the kinesin molecules, which we know are irreversibly bound to the surface, are almost certainly bound directly to the glass, as depicted in Fig. 1A, since we know that kinesin does not bind to casein (at least in solution). Also, since the single-motor assays can be performed when proteins other than casein are used to coat the glass surface (15, 25), it is unlikely that the binding of kinesin to the glass surface occurs by a specific interaction with casein.

Our technique for measuring kinesin's flexibility should also work for myosin, whose torsional flexibility has not been quantified. Qualitative evidence for torsional flexibility of myosin comes from electron microscopic observations that both of the myosin heads can bind the same actin filament *in vitro* (13); as pointed out by Craig *et al.* (13) this means that the two identical myosin heads, which, like kinesin, face in opposite directions because of the twofold rotational symmetry, must undergo a relative rotation (swivel) of 180° for them both to assume the translational similarity necessary for stereospecific binding to the one filament. The movement of actin filaments in opposite directions along oriented arrays of myosin molecules (26, 27) may also indicate torsional flexibility, though it is possible that these observations simply reflect the twofold symmetry of the two heads. Some degree of torsional flexibility is necessary for myosin to bind stereospecifically to consecutive action monomers on the helical actin filament.

What is the structural basis for kinesin's flexibility? Since the direction a kinesin molecule translates a microtubule is determined by the direction of the microtubule's long axis, the orientation of the force-generating power stroke must be determined by the orientation of the microtubule. Therefore, the compliant torsional spring, the swivel, must lie between the site of force generation within the motor domain and the other end of the molecule which is attached to the glass

surface. We do not know where in the motor the compliance is located. The 56-nm-long coiled-coil rod domain (7) comprises approximately three complete turns, each with a pitch of 18 nm (28); it is unlikely that the coiled coil could be twisted and untwisted through another two complete turns. More likely, the proteolytically susceptible neck region mentioned in the Introduction is highly disordered and therefore highly flexible. Irrespective of the physical location of the swivel, the remarkably high flexibility of kinesin suggests that kinesin may be described as a pair of motors at the end of a "piece of thread" as hypothesized for myosin by H. E. Huxley (9). The flexibility is probably vital for force generation: it is possible that the reason why the kinesin head alone cannot move (6, 29) is that the swivel is missing.

Our finding that movement is independent of microtubule orientation greatly simplifies the interpretation of *in vitro* motility assays in which the orientation of kinesin on substrates cannot easily be manipulated or determined. While our experiments were performed only at low loads (viscous drags forces $\ll 1$ pN), it is difficult to imagine how force generation could strongly depend on orientation given the existence of such a compliant element between the motor and the substrate.

Our results show that it is impossible to measure the single-motor force of kinesin by using the centrifuge microscope assay described by Hall *et al.* (30). The reason is that in their gliding assay the sperm's head, which provides the inertial force, is located at the minus end of the microtubules, and therefore leads because kinesin is a plus-end directed motor. If the sperm is moved by a single motor we expect the centrifugal force to rotate the sperm about the motor so that the head is at the greatest radius. The inertial force will then augment, rather than oppose, the motor force. Thus the force reported by Hall *et al.* (30) cannot be the single-motor force.

The degree of freedom introduced by the rotational flexibility of kinesin will increase the efficiency of motor-driven organelle movement in the following ways. First, the flexibility should accelerate the rate at which a kinesin-coated organelle binds to a microtubule: the correct alignment of a kinesin head for stereospecific binding to a microtubule will be achieved much more rapidly by rotation of kinesin's head than by rotation of the entire organelle. The potential acceleration of binding by this mechanism is large because the rotational diffusion coefficient is inversely proportional to diameter cubed: the 10-nm-long kinesin head will rotate diffusively $\approx 10,000$ times more quickly than a 200-nm-diameter organelle. Second, the flexibility should allow several randomly oriented motors on an organelle to work together: the motors need not be in highly oriented arrays like those found in muscle and cilia to cooperate in the movement of an organelle. Thus nearly 100% of the motors on the surface of an organelle that can reach the microtubule should be able to bind and exert force. By maximizing the number of motors and therefore the force pulling an organelle, kinesin's torsional flexibility compensates for the extremely low mobility of organelles in cytoplasm (31).

We especially thank Mr. F. Gittes for help with the hydrodynamic

modeling. We also thank Drs. A. M. Gordon, B. Hille, E. Meyhöfer, and S. Ray, and Messrs. S. Baek, B. Mickey, and F. Gittes for comments on the manuscript. This work was supported by the National Institutes of Health (AR40593) and the Alfred P. Sloan Foundation. J.H. is a Pew Scholar in the Biomedical Sciences.

1. Brady, S. T. (1985) *Nature (London)* **317**, 73–75.
2. Vale, R. D., Reese, T. S. & Sheetz, M. P. (1985) *Cell* **42**, 39–50.
3. Amos, L. A. (1987) *J. Cell Sci.* **87**, 105–111.
4. Ingold, A. L., Cohn, S. A. & Scholey, J. M. (1988) *J. Cell Biol.* **107**, 2657–2667.
5. Yang, J. T., Laymon, R. A. & Goldstein, L. S. B. (1989) *Cell* **56**, 879–889.
6. Kuznetsov, S. A., Vaisberg, Y. A., Rothwell, S. W., Murphy, D. B. & Gelfand, V. I. (1989) *J. Biol. Chem.* **264**, 589–595.
7. Hirokawa, N., Pfister, K. K., Yorifuji, H., Wagner, M. C., Brady, S. T. & Bloom, G. S. (1989) *Cell* **56**, 867–878.
8. Scholey, J. M., Heuser, J., Yang, J. T. & Goldstein, L. S. B. (1989) *Nature (London)* **338**, 355–357.
9. Huxley, H. E. (1969) *Science* **164**, 1356–1366.
10. Mendelson, R. A., Morales, M. F. & Botts, J. (1973) *Biochemistry* **12**, 2250–2255.
11. Thomas, D. D., Seidel, J. C., Hyde, J. S. & Gergely, J. (1975) *Proc. Natl. Acad. Sci. USA* **72**, 1729–1733.
12. Offer, G. & Elliot, A. (1978) *Nature (London)* **271**, 325–329.
13. Craig, R., Szent-Györgyi, A. G., Beese, L., Flicker, P., Vibert, P. & Cohen, C. (1980) *J. Mol. Biol.* **140**, 35–55.
14. Yguerabide, J., Epstein, H. F. & Stryer, L. (1970) *J. Mol. Biol.* **51**, 573–590.
15. Howard, J., Hudspeth, A. J. & Vale, R. D. (1989) *Nature (London)* **342**, 154–158.
16. Howard, J., Hunt, A. J. & Baek, S. (1993) *Methods Cell Biol.* **39**, 137–147.
17. Hyman, A., Drechsel, D., Kellogg, D., Salser, S., Sawin, K., Steffen, P., Wordeman, L. & Mitchison, T. (1991) *Methods Enzymol.* **196**, 478–485.
18. Sheetz, M. F., Block, S. M. & Spudich, J. A. (1986) *Methods Enzymol.* **134**, 531–544.
19. Papoulis, A. (1984) *Probability, Random Variables, and Stochastic Processes* (McGraw-Hill, New York), 2nd Ed., pp. 341–342.
20. Brennen, C. & Winet, H. (1977) *Annu. Rev. Fluid Mech.* **9**, 339–398.
21. Reif, F. (1965) *Fundamentals of Statistical and Thermal Physics* (McGraw-Hill, New York).
22. Beese, L., Stubbs, G. & Cohen, C. (1987) *J. Mol. Biol.* **194**, 257–264.
23. Jeffrey, D. J. & Onishi, Y. (1981) *Q. J. Mech. Appl. Math.* **34**, 129–137.
24. Miller, R. H. & Lasek, R. J. (1985) *J. Cell Biol.* **101**, 2181–2193.
25. Block, S. B., Goldstein, L. S. B. & Schnapp, B. J. (1990) *Nature (London)* **348**, 348–352.
26. Toyoshima, Y. Y., Toyoshima, C. & Spudich, J. A. (1989) *Nature (London)* **341**, 154–156.
27. Sellers, J. R. & Kachar, B. (1990) *Science* **249**, 406–408.
28. Phillips, G. N. (1992) *Proteins* **14**, 425–429.
29. Yang, J. T., Saxton, W. M., Stewart, R. J., Raff, E. C. & Goldstein, L. S. B. (1990) *Science* **249**, 42–47.
30. Hall, K., Cole, D. G., Yeh, Y., Scholey, J. M. & Baskin, R. J. (1993) *Nature (London)* **364**, 457–459.
31. Luby-Phelps, K., Castle, P. E., Taylor, D. L. & Lanni, F. (1987) *Proc. Natl. Acad. Sci. USA* **84**, 4910–4913.